# Assessment of Mental Fatigue in Healthy Participants During Extended BCI-HMD Sessions

N. Evetović, R. Rosipal, A. Polyanskaya, Z. Rošťáková and L.J. Trejo

Abstract—Prolonged use of brain-computer interfaces (BCIs) with virtual reality (VR) via head-mounted displays (HMDs) induces mental fatigue, potentially neurorehabilitation. This study examines EEG-based fatigue markers in healthy participants during extended BCI-HMD sessions. Fatigue was classified using N-way Partial Least Squares (N-PLS) with linear discriminant analysis, achieving 82.42% (±7.5) accuracy. N-PLS components revealed spatialspectral patterns in occipital and sensorimotor alpha activity. Temporal trajectories indicated progressive fatigue accumulation during sessions. Results demonstrate the feasibility of EEG-based fatigue monitoring for optimizing BCI-HMD post-stroke neurorehabilitation.

#### I. Introduction

Integrating brain—computer interfaces (BCIs) with virtual reality (VR) via head-mounted displays (HMDs) has a strong potential for post-stroke motor neurorehabilitation by enabling motor imagery (MI) training in immersive, ecologically valid environments. However, mental fatigue poses a major challenge to long-term BCI-HMD use, degrading MI performance and user engagement.

Mental fatigue is a complex cognitive state marked by reduced attention and increased effort during sustained tasks. While often assessed subjectively, EEG-based biomarkers, such as increased theta and alpha amplitude, offer objective indicators of fatigue progression [1]. Previous studies have examined these markers [2], [3], but little is known about their evolution during extended BCI-HMD use.

This study investigates neural markers of mental fatigue during long-term BCI-HMD VR sessions in healthy participants. Using N-way Partial Least Squares (N-PLS), we extracted latent EEG patterns associated with fatigue induced by sustained MI. The objective of this work is to contribute to the design of adaptive, real-time BCI-HMD systems tailored for practical use in post-stroke motor neurorehabilitation.

## II. MATERIALS AND METHODS

Experiment Design

The study employed a structured experimental design to investigate fatigue dynamics in a neurorehabilitation setting, particularly when using MI. Participants followed pre-session guidelines to minimize baseline fatigue and engaged in three sessions: a Mirror box session, a VR motor imagery session, and a Control session. Continuous

EEG recordings captured neural activity using the previously developed BCI-HMD system [4], with pre- and post-task assessments enabling analysis of sustained cognitive load and mental fatigue effects.

The experiment involved pre- and post-session resting state EEG recordings with eyes closed (EC) and eyes open (EO), a continuous performance test (CPT), and fatigue and cybersickness related questionaries.

EEG data were captured using the wireless g.Nautilus PRO FLEXIBLE system, an FDA-cleared device equipped with 32 Ag/AgCl wet EEG electrodes arranged according to the international 10-20 system; the HMD utilized was an autonomous Oculus Quest 2 (Meta Platforms, Inc.) headset and a publicly available software OpenViBE was used to interconnect these components.

EEG data were initially collected from 15 participants during the mirror box experiment. Due to dropouts, data was collected from 9 participants in the VR session and 10 in the Control session, with 8 completing all three sessions. One subject was excluded due to excessive artifacts, resulting in 7 subjects included in the final analysis.

Both VR and control sessions had 3 blocks of 25 trials. During the VR session, participants engaged in a MI paradigm, where they mentally imagined gestures without any physical movement when prompted by a voice command. Each trial consisted of resting state that lasted 20s and is used to set a threshold for the motor imagery phase. Throughout the trial, EEG signals were continuously monitored via the BCI-HMD system. When the required neural patterns were detected, a virtual arm animation was triggered, reaching toward an object, as illustrated in Fig. 1. If no activation was detected, the trial was automatically terminated after 20 seconds. After the motor imagery phase there was a 2-7s pause. Therefore, in total the trial lasted approximately 50s and each session lasted around one hour.



Figure 1. Patient grasping the cup in virtual reality

The control condition featured the same visual stimuli, however participants passively observed the scenario, with random trials marked as successful to control visual engagement. The probability of successful trials in the control session was 0.3, 0.4 and 0.35 for each block respectively.

## N-way Partial Least Squares Method

N-PLS is a supervised machine learning method that extends traditional PLS by projecting the multi-way input  $X \in \Re^{n \times I_1 \times I_2 \times ... \times I_N}$  and response arrays  $Y \in \Re^{n \times I_1 \times I_2 \times ... \times I_M}$  onto a lower-dimensional latent space that captures the maximum covariance between them [5]. In our study, the tensor X captures the multi-dimensional EEG data across time, frequency, and spatial modes. The Y matrix represents the class-membership labels or associated class information. For resting state EEG data we separated the harmonic and aperiodic components of the amplitude spectrum using the IRASA method [6].

This was performed on every 2-second segment of EEG data using a sliding window of 500 milliseconds.

After the extraction of a sub-set of k N-PLS latent variables  $T \in \mathbb{R}^{n \times k}$  the two-class linear discriminant analysis was applied to classify low- and high-levels of mental fatigue.

### III. RESULTS

To discriminate between low and high mental fatigue for each subject individually, artifact-free resting-state eyes-open (EO) EEG data collected before (low-fatigue class i.e. 0) and after (high-fatigue class i.e. 1) VR motor imagery and control sessions were combined. We applied 5-fold cross-validation to the combined dataset, performing 4-factor N-PLS on each fold. Applying the trained model on the test set across folds yielded an average classification accuracy of 82.42% (±7.5) across the seven subjects. The resulting factors were averaged across folds to obtain generalized components that are used for prediction of fatigue during the sessions. To avoid overfitting, we manually selected the optimal number of atoms for each subject based on performance across folds.

To illustrate the model performance, Fig. 2 shows the predicted N-PLS output values and true fatigue labels for subject 05 on the fold 1 test set.

We analyzed the latent variables (components) extracted by the N-PLS to gain insight into the underlying representations learned by the model. Each factor comprises weights distributed across the spatial and frequency dimensions, reflecting how the model leveraged different brain regions and spectral bands. In Fig. 3, we present the frequency weights alongside the corresponding spatial topographies for each of three selected N-PLS components for subject 05.

The frequency and spatial profiles of the extracted N-PLS components reveal distinct neurophysiological patterns associated with fatigue levels discrimination. The first latent factor exhibits a prominent spectral peak centered around 8.7 Hz, with the corresponding topographic weights predominantly localized over the

occipital region. The second factor is characterized by a positive peak at 8.3 Hz and a notable negative deflection at 11.7 Hz. Spatially, this component is primarily distributed over the left central region, with the strongest weights near the C3 electrode. The third factor shows a mild negative dip from 6.8 to 7.8 Hz followed by a peak at 9.7 Hz, with the topographic distribution focused over the occipital area with a slight lateralization to the right hemisphere.

To further interpret the neurophysiological basis of the N-PLS components, we examined the harmonic spectra of real EEG data from Subject 05 shown in Fig. 4 and 5. Notably, at the O1 electrode and neighboring parietal and occipital EEG channels, the most pronounced difference between the pre- and post-resting-state conditions was observed at 8.7 Hz, aligning with the peak frequency captured in the first N-PLS component. This suggests that changes in occipital alpha amplitude, particularly in the left hemisphere, contribute significantly to the model's discriminative capability.

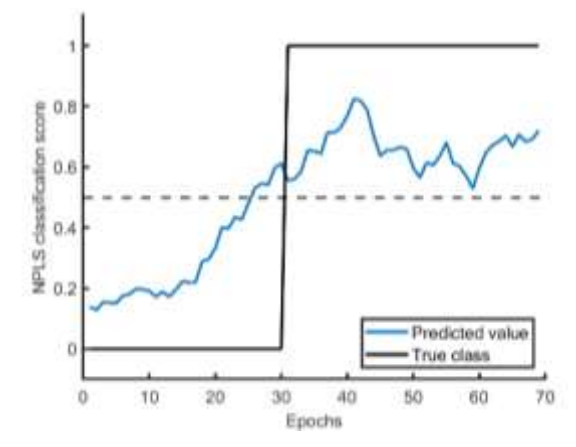


Figure 2. Comparison of predicted output values and true fatigue levels (low and high) for subject 05 on fold 1 test set, obtained using a N-PLS model trained on combined resting-state eyes-open EEG data collected before and after VR motor imagery and Control sessions.

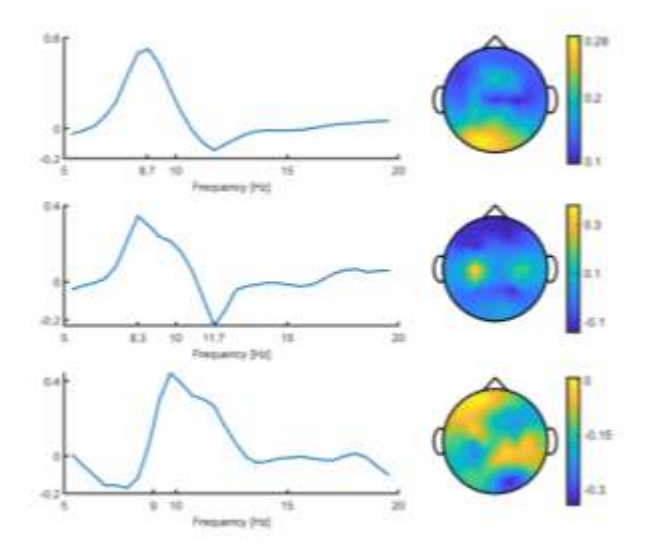


Figure 3. Frequency weights and topographies for the three latent variables of the N-PLS models of Fig.1. Each component illustrates the spectral and spatial features the model uses to discriminate between low-and high-fatigue states for subject 05.

At C3, located over the left sensorimotor cortex, we observed a leftward shift in the alpha peak frequency, reflecting a slowing of alpha activity, a phenomenon well-documented in fatigue-related EEG literature. Specifically, frequencies around 8.3 Hz and 11.7 Hz, highlighted in the second N-PLS component, correspond to the most substantial divergence in the slope of the alpha peak between conditions, reinforcing the component's relevance to changes in the sensorimotor cortical areas caused by fatigue.

Lastly, over the right parieto-occipital region—particularly at electrodes O2, PO8, and P8—spectral analysis revealed both an increase in alpha amplitude and a leftward shift of the alpha peak, with the pre-resting state condition alpha maximum centered at 9.7 Hz. This pattern aligns with the third N-PLS component, which captures a subtle reduction around 6.8–7.8 Hz and a peak at 9.7 Hz, localized over the right occipital scalp. These observations collectively provide physiological grounding for the extracted N-PLS components and help explain the specific spectral and spatial characteristics identified by the model.

Following the analysis of latent variables and the evaluation of classification performance on the test set, the trained N-PLS models were applied separately to the continuous data from each session. The aim was to investigate whether the models could capture the temporal evolution of mental fatigue and whether they could be used to visualize gradual fatigue accumulation over time.

Fig. 6 and 7 present the predicted fatigue trajectories for subject 05, with the percentage of artifact-free EEG electrodes shown above each time point to indicate EEG signal quality. Importantly, predictions were performed on data containing artifacts, to mimic realistic conditions under which this method would be deployed in an online BCI-HMD neurorehabilitation setting. In such applications, real-time mental fatigue monitoring must operate on raw or minimally processed EEG signals,

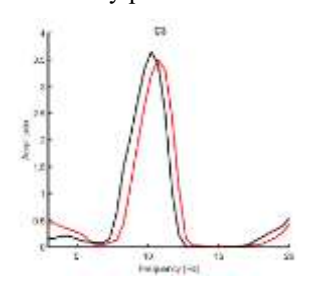


Figure 4. Harmonic spectra of EEG signal at electrode C3 for subject 05.

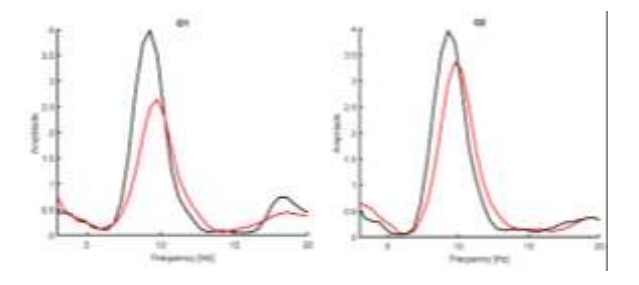


Figure 5. Harmonic spectra of EEG signal at electrodes O1 (left) and O2 (right) for subject 05.

as artifact removal and reduction of EEG electrodes is not feasible during live sessions.

This approach thus evaluates the practical applicability of the proposed method in ecologically valid, real-world scenarios. For each of the seven subjects, we computed the mean N-PLS classification scores from the VR motor imagery and Control sessions to illustrate the temporal evolution of predicted fatigue levels throughout each session. Fig. 8 displays each subject's predicted mental fatigue scores across multiple time points. Each plot shows eleven predicted fatigue values per subject: the first corresponds to the pre-session rest-state measurement, the next nine represent predicted fatigue scores across three experimental blocks (three values per block), and the final value reflects mental fatigue prediction at the post-session resting state condition.

For all subjects, there is a noticeable increase in predicted mental fatigue scores toward the fatigued state by the end of the experiment, with occasional temporary decreases. This trend is evident across both experimental conditions, indicating that the N-PLS model effectively captures the gradual increase in mental fatigue over time.

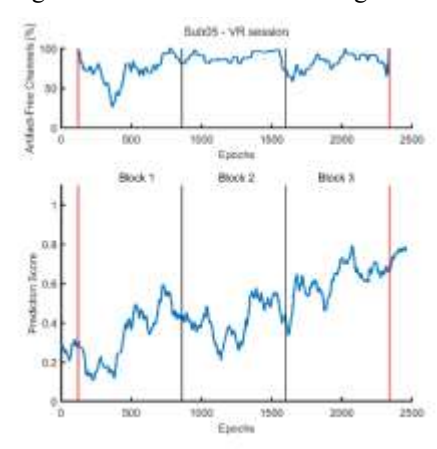


Figure 6. N-PLS-based mental fatigue classification scores across VR session segments (pre, blocks 1–3, post) and the corresponding percentage of artifact-free EEG electrodes for subject 05.

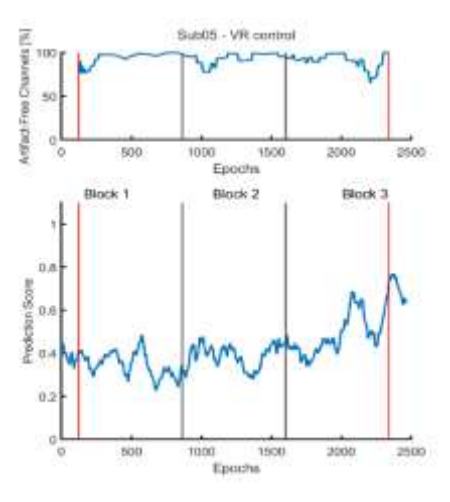


Figure 7. N-PLS-based mental fatigue classification scores across the Control session segments (pre, block 1–3, post) and the corresponding percentage of artifact-free EEG electrodes for subject 05.

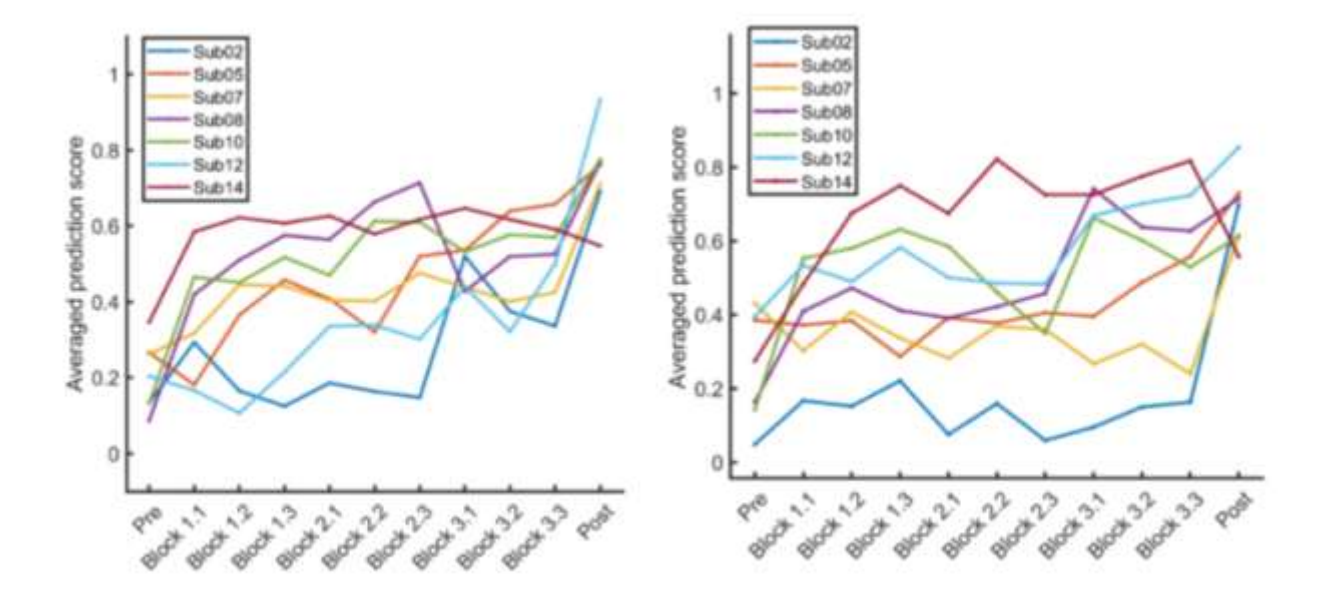


Figure 8. Predicted mental fatigue levels across the VR motor imagery (left) and Control (right) sessions for seven subjects, based on N-PLS classification scores.

#### IV. CONCLUSION

This study demonstrates the feasibility of using EEGbased biomarkers to detect mental fatigue during extended sessions involving brain-computer interfaces integrated with virtual reality head-mounted displays (BCI-HMD). By applying N-way Partial Least Squares (N-PLS) with linear discriminant analysis, we achieved an average classification accuracy of 82.42% across seven subjects in distinguishing between low- and high-fatigue states. The extracted latent components revealed neurophysiological patterns—particularly in occipital and sensorimotor alpha activity—corresponding to fatigue accumulation. Temporal tracking across sessions confirmed the progressive nature of mental fatigue, even under artifact-prone, real-world conditions. However, predicted fatigue scores during VR motor imagery are not more pronounced than in the Control session. These findings support the integration of real-time fatigue monitoring into adaptive BCI-HMD systems, potentially enhancing their effectiveness and usability in post-stroke motor neurorehabilitation.

## ACKNOWLEDGEMENT

Funded by the EU NextGenerationEU through the Recovery and Resilience Plan for Slovakia under the project No. 09I03-03-V04-00205 (Z.R.) and project No. 09I03-03-V04-00443 (R.R.). N.E. received funding from the HORIZON-MSCA-2022-DN, 101118964-DONUT project.

## REFERENCES

- [1] Y. Tran, A. Craig, R. Craig, R. Chai, and H. Nguyen, "The influence of mental fatigue on brain activity: Evidence from a systematic review with meta-analyses," *Psychophysiology*, vol. 57, no. 5, p. e13554, May 2020, doi:10.1111/psyp.13554.
- [2] L. J. Trejo, K. Kubitz, R. Rosipal, R. L. Kochavi, and L. D. Montgomery, "EEG-Based Estimation and Classification of

- Mental Fatigue," *Psychology*, vol. 06, no. 05, pp. 572–589, 2015, doi: 10.4236/psych.2015.65055.
- [3] H. Yaacob, F. Hossain, S. Shari, S. K. Khare, C. P. Ooi, and U. R. Acharya, "Application of Artificial Intelligence Techniques for Brain–Computer Interface in Mental Fatigue Detection: A Systematic Review (2011–2022)," *IEEE Access*, vol. 11, pp. 74736–74758, 2023, doi:10.1109/ACCESS.2023.3296382.
- [4] R. Rosipal, Š. Korečko, Z. Rošťakova, N. Porubcová, M. Vankó, and B. Sobota, "Towards an Ecologically Valid Symbiosis of BCI and Head-mounted VR Displays," in 2022 IEEE 16th International Scientific Conference on Informatics (Informatics), Poprad, Slovakia:IEEE, Nov. 2022, pp. 251–256. doi: 10.1109/Informatics57926.2022.10083479.
- [5] R. Bro, "Multiway calibration. Multilinear PLS," J. Chemom., vol. 10, no. 1, pp. 47–61, Jan. 1996, doi:10.1002/(SICI)1099128X(199601)10:1<47::AIDCEM400>3.0. CO;2-C.
- [6] H. Wen and Z. Liu, "Separating Fractal and Oscillatory Components in the Power Spectrum of Neurophysiological Signal," *Brain Topogr.*, vol. 29, no. 1, pp. 13–26, Jan. 2016, doi: 10.1007/s10548-015-0448-0.